International Journal of Engineering and Management Research e-ISSN: 2250-0758 | p-ISSN: 2394-6962
Volume-11, Issue-3 (June 2021)
www.ijemr.net https://doi.org/10.31033/ijemr.11.3.26

Comparative Analysis of Equivalent Material based on MFI

Mahesh Zope[1], Pratik Sonawane[2] and Deepti Marathe[3]
[1]Student, School of Polymer Engineering, MIT-WPU, Pune, INDIA
[2]Student, School of Polymer Engineering, MIT-WPU, Pune, INDIA
[3]Associate Professor, School of Polymer Engineering, MIT-WPU, Pune, INDIA

[1]Corresponding Author: mahesh.k.zope@gmail.com

ABSTRACT

Polymers of the same family show distinct behavior with each other and because of this, the end prediction after molding the part is very difficult. Simulations result does not always match the product. For close substitution in absence of exactly known material composition, the equivalent grade of the same MFI may be used. However, the MFI is a poor indicator of the rheological behavior to be comprehend for accurate simulation. This research analyzes the appropriate parameters for the rheology of polymers, in the same class that are appropriate.

Keywords— Injection Molding, Simulation, MFI

I. INTRODUCTION

In general, a higher MFI indicates a lower material viscosity, and when comparing polymers of the same class/family, a lower melt flow rate corresponds to a higher molecular weight. Melt flow rate is a measure of the ability of the material's melt to flow under pressure. Melt flow rate is inversely proportional to the viscosity of the melt at the conditions of the test that the viscosity for any such material depends on the applied force.

Polymer viscosity is affect by several factors, such as temperature, concentration, molecular weight, Shear-thinning behavior, molecular structure, shear elongation, and shear rate. Melt flow rate is an indirect measure of molecular weight.

However, MFI takes no account of the shear, shear rate, or shear history and as such is not a good measure of the processing window of a polymer. It is a single-point viscosity measurement at a relatively low shear rate and temperature. It was often that MFI gives a 'dot' when actually what is need is a 'plot' for the polymer processors. MFI additionally does not take account of long-chain branching nor the differences between shear and elongation rheology. Therefore, two polymers with the same MFI will not behave the same under any given processing conditions.

The relationship between MFI and temperature can be use to obtain the activation energies for polymers [12]. The activation energies developed from MFI values has the advantage of simplicity and easy availability. The concept of obtaining activation energy from MFI can be extended to all processing polymers as well wherein there exists an anomalous temperature dependence of melt viscosity leading to the existence of two distinct values of activation energies for each copolymer[1]. Ratio between two melt flow rate values for one material at different gravimetric weights are often used as a measure for the broadness of the molecular weight distribution.

E.E. Ferg, L.L. Bolo studied to establish a correlation between the variable melt flow index (VMFI) values of molten polypropylene (PP) with different piston-load masses using a standard MFI analyzer as well as the effect of flow characteristics of the polymer [2]. While working finding are correlation between flow characteristic and average molecular weight distribution of good repeatability could be achieve with the technique giving an indication of the polymer's flow properties over a small range of variable applied pressures. The study showed that one should not only rely on a single MFI value of a polymer to characterize the flow properties,

Krzysztof Wilczynski and Przemysław Narowski studied the effect of material characteristics and runners layout geometry on the filling imbalance in geometrically balanced injection molds [3]. They concluded that, the velocity/shear rate distribution and the heat transfer conditions from the polymer melt to the mold are two main factors affecting the filling imbalance in addition when the flow rate increases, the filling imbalance increases since the non-linearity of velocity/shear rate distribution also increases.

Xiaolei Xu, Jizhong Chen and Lijia An studied shear thinning behavior of linear polymer melts under shear flow via non-equilibrium molecular dynamics [4]. They concluded that In the non-Newtonian regime $\dot{\gamma}>\tau 0-1$, the shear dependence of viscosity exhibits a crossover at a shear rate $\gamma\dot{c}$, under which the power law is dependent on chain length while above which independent of chain length. In addition, they concluded that the characteristic shear rate $\dot{\gamma}c$ is found weakly dependent on chain length.

Chau-Chyun Chen, Tim Bremner, done Research on Polymer Viscous Flow Activation researched quantifying Relationships among the Molecular Weight

Distribution, Non-Newtonian Shear Viscosity, and Melt Index for Linear Polymers [5]. They are able to relate the flow curve and MWD using either a modified Carreau-Yasuda or Bersted partition model, the MI and MWD use Bremner and Rudin's model, and the flow curve and the MI using Rohlfing and Janzen's model. Both the modified Carreau-Yasuda and Bersted models successfully correlate the MWD and flow curve for the three LLDPEs, producing four parameters. Also, they able to compute the MIs accurately using Rohlfingand Janzen's fluid mechanics model and flow curves predicted by either the modified Carreau-Yasuda or Bersted model.

Yan Lou , Qunan Lei, and Gang Wu done research on polymer viscous flow activation energy and non-Newtonian index model based on feature size [1]. They concluded that at the microscopic scale, the viscous flow activation energy of PMMA decreases with the feature size, while the viscous flow activation energy of the crystalline polymer PP and HDPE increases with the die diameter. Also, they concluded that the non-Newtonian index of the three polymer materials decreases with the feature size within the microscopic scale, while it increases or does not change with the feature size within the macroscopic scale.

In this study, we are trying to identify the effect on part by material which is having differences in rheological parameters like viscosity, thermal conductivity, and viscoelasticity and so on, which is used as an input for the simulation [6][7]. We considered 3 grade for simulation of ABS family which have the same MFI 22 gm/10min (220,10), as follows:

ABS-A: Toyolac 125 Toray
ABS-B: Sinkral L320 Polimeri Europa
ABS-C: LG ABS HG173 LG Chemicals

II. EXPERIMENTAL WORK

The Experimental work was divide into two steps. The first one is to the understanding of the rheological difference in 3 grades, which have the same MFI 22g/10min (220,10), In the second step, An analysis of the product the experimental methodologies, exploring the main aspects to show the difference in result outcome of the product.

2.1 Materials

We have used three different grades of ABS, which is available in moldex3D library, with consideration of reference polymer to compare the research results with recently performed experimentations and other simulations [8][9]. We selected equivalent grade materials based on MFI 22g/10min (220,10) as follows:

ABS-A: Toyolac125 Toray
ABS-B: Sinkral L320 Polimeri Europa
ABS-C: LG ABS HG173 LG chemical

The above 3 materials grades have been chosen as they are available for simulation in the material library of the MOLDEX-3D software.

2.1.1 Viscosity

At both sufficiently high and very low shear rates, A viscosity of a polymer system is independent of the shear rate [6][10]. At high shear rates, polymers are entirely disentangle and the viscosity value of the system plateaus at $\eta\infty$, the infinite shear viscosity. At low shear rates, the shear is too low to impede by entanglements and the viscosity value of the system is $\eta 0$, the zero shear rate viscosity. The value of $\eta\infty$ represents the lowest viscosity attainable and may be orders of magnitude lower than $\eta 0$, depending on the degree of shear thinning. viscosity is plotted against shear rate in a log-log plot, where the linear region is the shear thinning regime and can be expressed using the modified Cross model [8]:

Cross model

$$\eta = \frac{\eta_0}{1 + \left[\frac{\eta_0 \times \dot{\gamma}}{T^*}\right]}$$

$$\eta_0 = D_1 exp\left[\frac{-A_1(T - T_c)}{A_2 + (T - T_c)}\right]$$

$$T_c = D_2 + D_3 P$$

$$A_2 = \tilde{A}_2 + D_3 P$$

Where,

$\eta 0$ = the zero-shear rate viscosity.
$\eta\infty$ = the lowest shear rate viscosity attainable
τ^* = onset of shear-thinning
D1 = Height onset of shear-thinning
D2 = Non-flowing temperature
D3 = Pressure effect
A1 = Temperature sensitivity which

Refer below figure which shows the comparison of viscosity plot at a temperature of 230°C MFI 22 gm/10min (220,10) [6]. The plot includes the three grades which exhibit different natures at a specific shear rate. ABS-A shows a higher viscosity than ABS-B and ABS-C. With consideration of low shear rate points numbered 1, 2, & 3 show a difference in viscosity which may results in flow hesitation, stress mark, short fill, and flow-related issues [6]. On another hand, at high shear stress, viscosity is the same between ABS-B and ABS-C but they differ from ABS-A, which means ABS-A will fill faster than ABS-B and ABS-C. Based on this fill time, the cycle time is also shorten. The behavioral prediction will be monitor by simulation.

e-ISSN: 2250-0758 | p-ISSN: 2394-6962
Volume-11, Issue-3 (June 2021)
https://doi.org/10.31033/ijemr.11.3.26

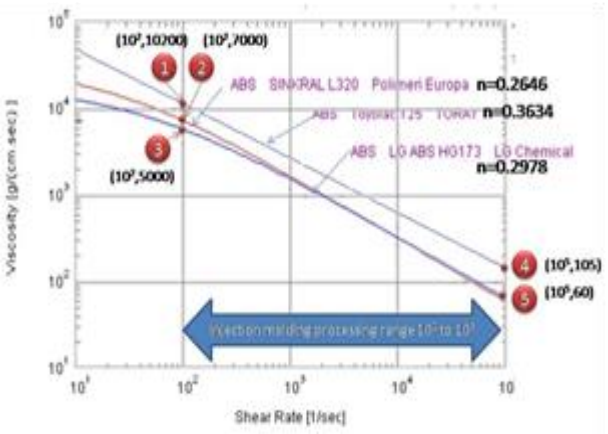

Figure 1: Viscosity Plot

2.1.2 PVT (Pressure-Volume-Temperature)

PVT diagram describes the specific volume as a function of pressure and temperature. The Specific volume increases with the temperature increasing. There is a thermal transition in the polymer. The primary amorphous transition of any polymer is known as its glass transition temperature, Tg. While Tg is not a sharp transition, the data from below and above Tg will show an intersection that is generally accepted as being Tg.

In the equilibrium state, ABS amorphous polymers have a random and entangled molecular orientation. An analogy behind the amorphous polymer is the "bundle of threads." for the flow of polymer by applying the energy, the forces between molecules/bond weaken and the channel gets brake. Besides, the uncoil and aligned the molecule the shear force exerting during the filling. At the end of melt flow, the molecules relax and return to a state of random orientation but Intermolecular forces continue to pull them closer together until the temperature drops enough to freeze them in place. These forces result in uniform shrinkage, but the relaxation effect causes significantly more contraction in the direction of flow.

This is the input to determine the dimensional change in volume due to thermal expansion or shrinkage. Refer below Plot, which shows the comparison of three Grades at 100 MPa and the variation between the plateaus is very less. the marginal difference of glass transition temperature Tg is here but the volumetric effect on the end may same.

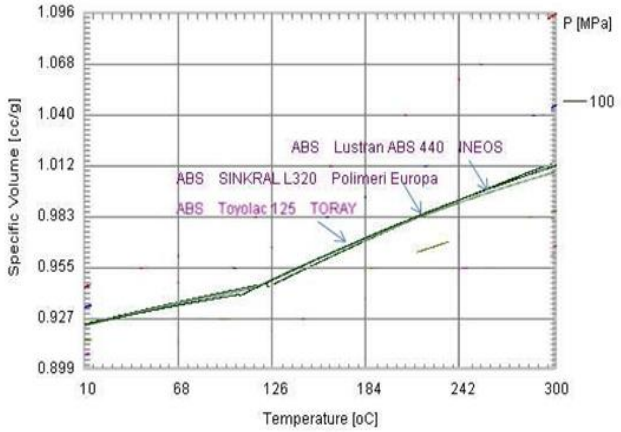

Figure 2: PVT Plot

ABS-A : Toyolac 125 Toray, Tg = 97 °C
ABS-B : Sinkral L320 Polimeri Europa Tg = 89.95 °C
ABS-C : LG ABS HG173 LG chemical Tg = 94.85 °C

2.1.3 Specific Heat

The specific heat is the amount of heat per unit mass required to raise the temperature by one degree Celsius. While comparing the data of ABS-A and ABS -C reflects the Straight behavior, which means the assumption is the behavior of material is same for the specified temperature, where as in ABS-B shows the tabulated data means actual/experimental data. This is resulting outcome is more realistic with ABS-B.

2.2 Product Design

The product used for the case study is fan plastic. The complete project of a fan executed in the CAD (Computer-Aided Design) Creo-2. In this product design, functional requirement is Geometry of the product refer below Figure 3, this drives the functional requirement of the assembly product/end product, which shows in fig 4.
The product size is

– Length : 240mm
– Width : 240mm
– Hight : 85mm

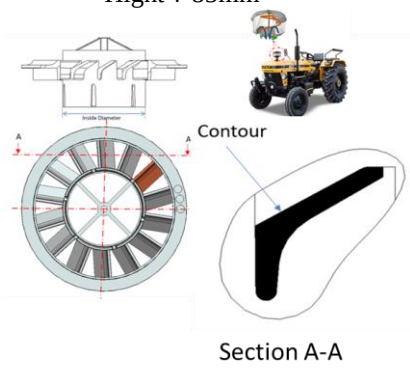

Figure 3: Product Design

2.3 Simulation Work

The complete simulation work of such fan executed in the moldex3D software (version R16). To know the effect of the various parameter we kept the process setting is the same for these simulations for three grade, refer below table [1].

2.3.1 Process Setting

In the simulation, we kept below process parameters, the same for three materials and evaluating the comparative study and there result [12][13].

Table 1: Process settings

Parameter	Value
Filling Time (s)	1.80
Melt Temperature (°C)	250.0
Mold Temperature (°C)	60.0
Injection Volume (cm3)	399.265
Packing Time (s)	12.00
VP Switch by filled volume (%)	98.00
Mold Opening Time (s)	5.00
Air Temperature (°C)	25.0
Cooling Time (s)	30.00
Cycle Time (s)	48.80

For the tool design, by studying the product geometry/shape, we design the suitable gate and runner design based on manufacturing possibility

The product design call for three-plate mold design, here the advantage with the three plate mold design is help to feed the art from center with four drop. The plate mold usually uses pinpoint gate so it detached easy from product and the runner can remove separately.

2.3.2 Cooling Layout

In consideration of Mold layout, the cooling channel is designed (refer image 4).

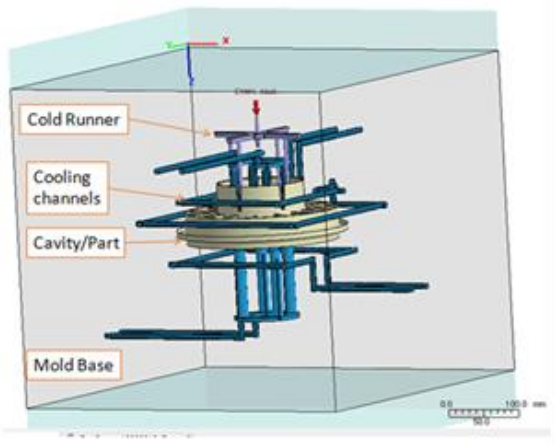

Figure 4: Tool Design

A Cooling Channel is typically use in a permanent mold die. These are the channel or area in the die where a fluid is flow, which is assume to have a constant temperature. The cooling channel used for thermal management of the process to prevent the overheating of the die and to control the solidification of the casting.

2.3.3 Runner Layout

A runner system directs the melt flow from the sprue to the mold cavities [3][14]. The runner design contributes in to the pressure, temperature and shear. Shear (frictional) heat generated within the melt while the material is flowing through the runner raises the melt temperature; affect the pressure also facilitating the flow.

The runner is designed as per suitable for three plate mold design.

2.3.4 Filling Pressure

Result observation against the filling Pressure is seen the viscosity of ABS-A is in higher than ABS-B and ABS-C that means ABS -A corresponds to a higher molecular weight or we can say required high activation energy [6][11]. The higher molecular weight corresponds to the filling pressure raise. We can see from table no 2, the pressure induced in the cavity to fill the part for ABS-A is higher than ABS-B and ABS-C. As per the viscosity plot of filling the cavity, viscosity effect is high.

Table 2: Simulation: filling pressure result

Parameters	Units	ABS -A : Toyolac Toray	ABS-B : Sinkral l320 Polimeri Europa	ABS-C : LG ABS HG173 Lg chemical
Filling Pressure Cavity+Runner	Mpa	91	50	56

The pressure distribution of the cavity is shown in different colors at the current instant. Based on the pressure drop and distribution. In Simulation result, we studied the pressure transmission situation in the part, runner system pressure drop which should not on the higher side, found non uniform flow in to the cavity, Avoid over packing and flashing of melt and in last Examined the extent of packing/holding (refer fig 5).

e-ISSN: 2250-0758 | p-ISSN: 2394-6962
Volume-11, Issue-3 (June 2021)
https://doi.org/10.31033/ijemr.11.3.26

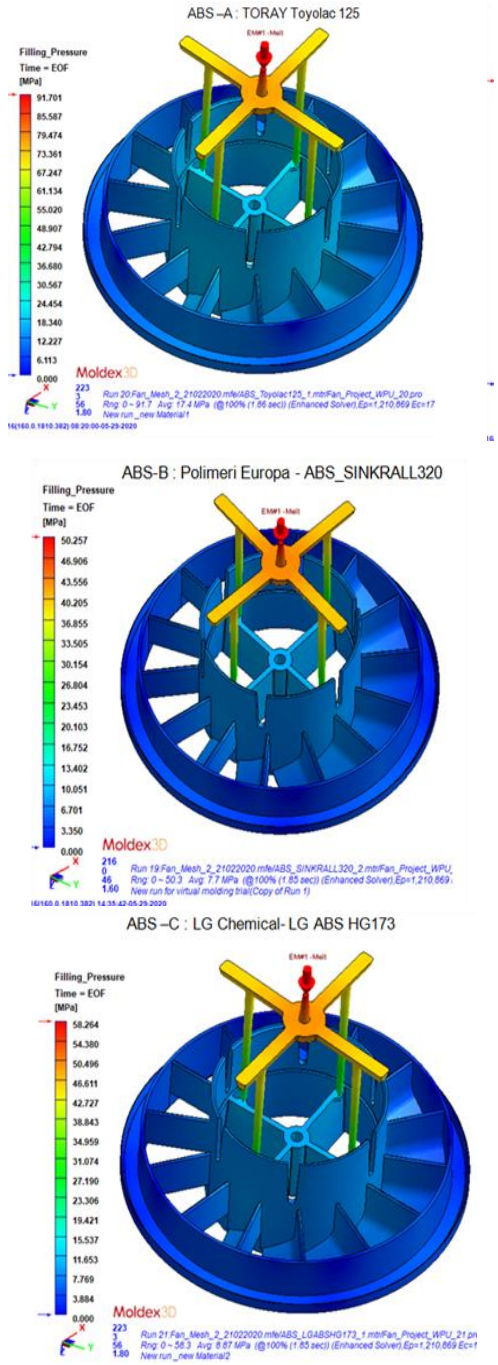

Figure 5: Simulation result of Filling Pressure in cavity

2.3.5 Filling - Melt Front Temperature

The melt front temperature is the indication of the temperature value of the plastic melt as it reaches the given point. This value indicates how heat is convey and dissipated during the molding phases. The prediction of shear heating melts front temperature [12]. The effect of shear heating for three grades shows distinct behavior (refer fig 6) and shear heating is happening near gate resign which shown in Fig 7 and shear heating in the runner will affect the density of the component and the required packing which may result in more shrinkage, reduction in mechanical property and defects in the component.

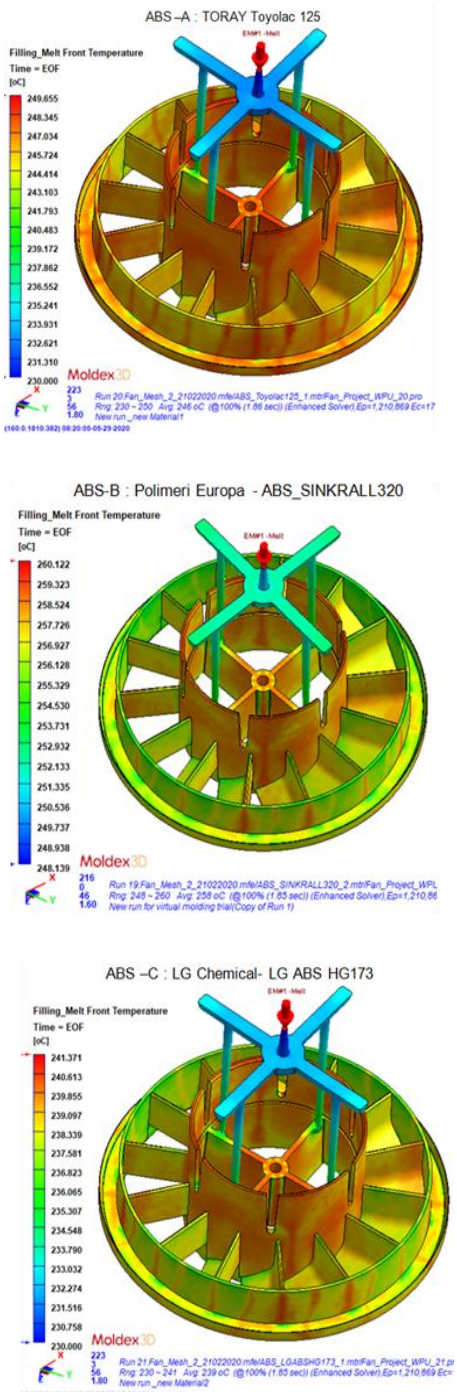

Figure 6: Simulation result of Melt front Temperature

e-ISSN: 2250-0758 | p-ISSN: 2394-6962
Volume-11, Issue-3 (June 2021)
https://doi.org/10.31033/ijemr.11.3.26

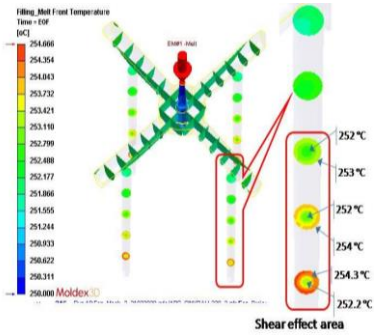

Figure 7: Simulation result of Melt front Temperature (Detailed)

2.3.6 Sprue Pressure

The result shows this sprue pressure is generate within the cavity. as per result observation, higher viscosity results in to higher sprue pressure, the ABS-1 shows high sprue pressure (112 MPa) than ABS-2 (71 MPa) and ABS-3 (69 MPa). Based on the sprue pressure, tonnage also changed. so this will mislead the end-user while selecting the molding machine.

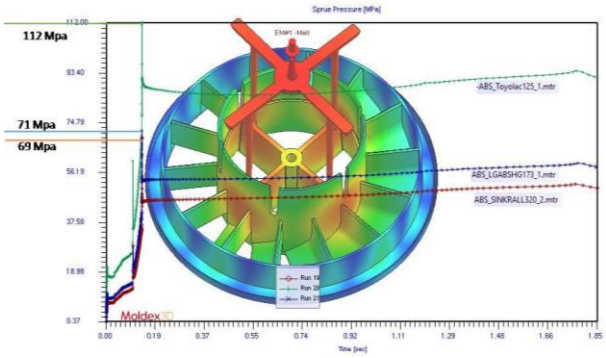

Figure 8: Simulation result of sprue pressure

Table 3: Simulation: filling pressure result

Parameters	Units	ABS -A : Toyolac Toray	ABS-B : Sinkral l320 Polimeri Europa	ABS-C : LG ABS HG173 Lg chemical
Sprue pressure	Mpa	112	69	71
Packing pressure	Mpa	70	38	44
Clamping Force	Ton	219	125	145

For any product, the sprue pressure and the tonnage is important for the selection of a machine and cost of the product. Now by seeing the results the clamping pressure is for ABS-A double than ABS -B &ABS-C. So this will mislead while mold machine selection.

2.3.7 Total Warpage

Total Displacement represents the summation of all displacement occurs from the time of the end of filling to the time while the temperature of the part reaches the room temperature [13]. It includes all factors affecting the behavior of warpage and the outcome of the combination of differential temperature effect, volumetric shrinkage, differential shrinkage effect, thermal induced stress. (Refer fig 9).

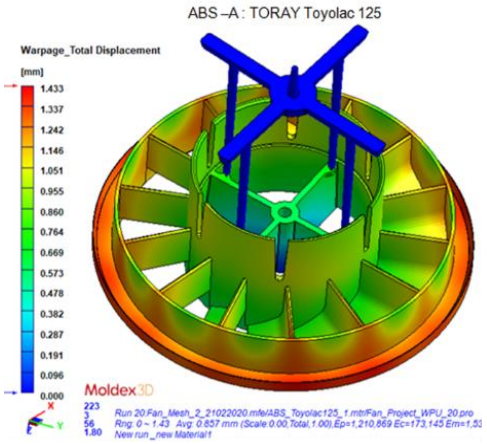

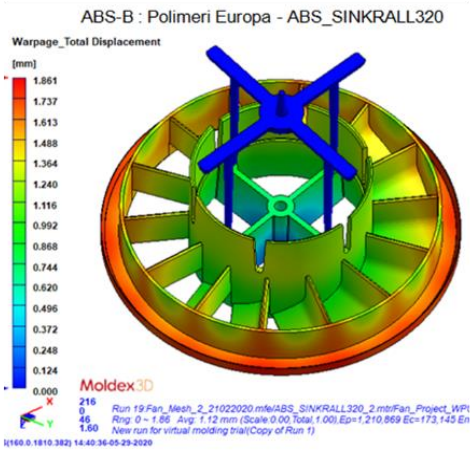

e-ISSN: 2250-0758 | p-ISSN: 2394-6962
Volume-11, Issue-3 (June 2021)
https://doi.org/10.31033/ijemr.11.3.26

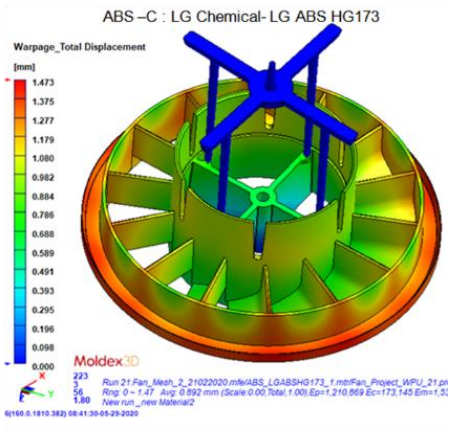

Figure 9: Simulation result of total warpage

Above results Show the length of the total displacement vector (All effects are considered) after the part is ejected at specific temperature. The value is relative to the model coordinate.

Table 4: Warpage Results

Parameters Displacement		Units	ABS -A: Toyolac Toray	ABS-B: Sinkral l320 Polimeri Europa	ABS-C: LG ABS HG173 Lg chemical
Warpage	Warpage X	mm	+1.3/-1.3	+1.7/-1.7	+1.3/-1.3
	Warpage Y	mm	+1.32/-1.3	+1.76/-1.74	+1.37/-1.36
	Warpage Z	mm	+0.8/-0.4	+1.00/-0.5	+0.85/-0.41
	Warpage total	mm	1.433	1.86	1.47
Differential Temperature Effect	Warpage X	mm	+0.3/-0.26	+0.39/-3.2	+0.298/-0.257
	Warpage Y	mm	+0.248/-0.242	+0.28/-0.75	+0.233/-0.232
	Warpage Z	mm	+0.167/-0.178	+0.193/-0.21	+0.166/-0.167
	Warpage total	mm	0.34	0.4	0.339
Differential Shrinkage Effect	Warpage X	mm	+1.088/-1.082	+1.48/-1.47	+1.137/-1.134
	Warpage Y	mm	+1.094/-1.087	+1.49/-1.48	+1.146/-1.137
	Warpage Z	mm	+0.65/-0.269	+0.89/-0.35	+0.696/-0.283
	Warpage total	mm	1.168	1.56	1.22

By analyze the product and dimension results is shown in above table no 4. The result comparison of differential temperature effect and differential shrinkage effect, the shrinkage effect is more contributing factor in the warpage, which means the molecular orientation, affect more in part. Because the flow front is not uniform, the geometry contribution is more. The molecular orientation is in the radial direction, which results in more shrinkage.

III. CONCLUSION

It has been observe that parameters, index flow, critical shear stress, and zero viscosity, as well as the thermal diffusivity and heat transfer coefficient strongly affect the filling. The effect is substantially dependent on the runner layout geometry as well as on the operating conditions, flow rate, and shear rate.

In the filling stage, the viscosity affects much in this stage. as per results, the pressure build to fill the part into the cavity is increases with high viscosity grade ABS-A than the ABS-B and ABS-C and account of temperature, the effect for the different grade show some amount of effect which can be identified in warpage differential temperature effect results. In some area, temperature zone shows the contribution towards the warpage which we identified in warpage differential result, it is small but it results in a significant effect.

In Simulation, the effect of viscosity (shear thinning behavior Slop n) affects the pressure in the cavity, which require filling. The slop also because of molecular weight that calls for the variation in tonnage for ABS-A is approximately double than ABS-B and ABSC. Therefore, this will miss leading the costing person while selecting a machine.

Therefore, MFI takes no account of the shear, shear rate, or shear history and intrinsically is not an honest measure of the processing window of a polymer. In the processing window, the viscosity, which differs in shear thinning and contribution of Shear-thinning, is much more in results variation. Therefore, two polymers with an equivalent MFI will not behave an equivalent under any given processing conditions.

REFERENCES

[1] Yan Lou, Qunan Lei, & Gang Wu. (2019). Research on polymer viscous flow activation energy and non-newtonian index model based on feature size. *Article ID 1070427*.

[2] E.E. Ferg & L.L. Bolo. (2013). *A correlation between the variable melt flow index and the molecular mass distribution of virgin and recycled polypropylene used in the manufacturing of battery cases*. DOI: 10.1016/j.polymertesting.2013.09.009.

[3] Krzysztof Wilczynski & Przemysław Narowski. (2019). Simulation studies on the effect of material characteristics and runners layout geometry on the filling imbalance in geometrically balanced injection molds. *Polymers, 11*, 639.

[4] Xiaolei Xu, Jizhong Chen, & Lijia An. (2014). Shear thinning behavior of linear polymer melts under shear flow via non-equilibrium molecular dynamics. *The Journal of Chemical of Chemical Physics, 140*, 174902.

[5] Chau-Chyun Chen, Tim Bremner, Kevin C. Seavey, Y. A. Liu, & Neeraj P. Khare. (2003). Quantifying relationships among the molecular weight distribution, non-Newtonian shear viscosity, and melt index for linear polymers. *Ind. Eng. Chem. Res.*, *42*, 5354-5362.
[6] Lukáš Satin & Jozef Bílik. (2016). Impact of viscosity on filling the injection mold cavity. *Slovak Uni. of Tech., Bratislava*, *24*, 113.
[7] Alexander Bakharev, David Astbury, Shishir Ray, Franco S. Costa, & Russell Speight. (2016). Effect of normal stresses on the results of thermoplastic mold filling simulation. *MATEC Web of Conferences*, *80*, 16004. DOI: 10.1051/matecconf/20168016004.
[8] Hyeyoung Shin & Eun-Soo Park. (2013). *Analysis of incomplete filling defect for injection-molded air cleaner cover using moldflow simulation*. Hindawi Publishing Corporation.
[9] Wilczy nski, K. & Narowski, P. (2019). Experimental and theoretical study on filling imbalance in geometrically balanced injection molds. *Polym. Eng. Sci.*, *59*, 599–604.
[10] Lei Zhong , Haihang Xu , Jizhao Liang , & Anping Liao. (2012). A new extensional viscosity model based on the cross model for polymer fluids. *Advanced Materials Research*, 415-417.
[11] Diego Alves de Miranda & André Lourenço Nogueira. (2018). Simulation of an injection process using a CAE tool: Assessment of operational conditions and mold design on the process efficiency. *Materials Research*, *22*(2), e20180564.
[12] Mr. G.V. Pujari, & Prof. Dr.V.R.Naik. (2015). Process parameters optimization for development of defect free injection molded components. *International Journal of Science, Technology and Management*, *4*(10), 56.
[13] Wu-Lin Chen, Chin-Yin Huang, & Ching-Ya Huang. (2013). Finding efficient frontier of process parameters for plastic injection molding. *Chen et al. Journal of Industrial Engineering International*, *9*, 25.
[14] Ranjit Singh & Jatinder Madan. (2014). Computer aided runner and gating system design from die-casting part model. In: *5th International & 26th All India Manufacturing Technology, Design and Research Conference*.
[15] Jian Wang. (2012). *PVT properties of polymers for injection molding, some critical issues for injection molding*. Dr. Jian Wang (Ed.), ISBN: 978-953-51-0297-7.